

---

# Effects of Drive Input Pulse and Heater Surface on the Uniformity of Bubble Jet Printheads

**K. Bühler, W. Pekruhn, S. Scherdel and W. Schullerus**  
**Inkjet Systems, Berlin, Germany**

---

## Abstract

An important aspect of print quality is the uniformity of the bubble growing process on the thermal heater elements within the bubble jet printhead. The bubble size primarily defines the volume of the expelled ink drop. The local and temporal stability of the bubble represent the uniformity of drop mass and drop velocity. Using an open pool test set-up with stroboscopic lighting and opaque or transparent waterbased fluids two major influences on the bubble uniformity are investigated—drive input pulse and heater surface. For a range of different drive input pulse powers and heater surface materials the effects on bubble uniformity will be reviewed. Experimental data will be given. The impacts on the bubble jet printhead design will be discussed.

## Introduction

The increasing number of personal computers creates a steadily growing demand for hardcopy printers. The motto on the PC field which can be characterized by ‘continuous improvement of performance and dramatically falling consumer prices’ also applies for the printer sector.

None of today’s print technologies on the marketplace meets this challenge better than the bubble-jet principle. In other words, none of them gives the end users better performance for less money.

Since the release of the first bubble-jet (BJ) printers eight years ago—Canon BJ80<sup>1</sup>, HP Think Jet<sup>2</sup>—major improvements have been achieved: Increase of resolution from 180 dpi to 300 dpi (typically), plain paper capability, better inks (less kogation, faster drying, higher optical density etc.), higher printing speed, color printing, and the introduction of a new generation of portable printers.

The current spectrum of BJ-printers includes machines for the office like the *IS92* and its color version

*IS92c* by Inkjet Systems, as well as portables like the *Diconix 701* by Kodak, which is equipped with a *DPH50-printhead* by Inkjet Systems. This printhead is available for OEMs too.

Commercial success of the BJ principle is based on small dimensions of the actuators (thin film resistors) and use of modern semiconductor mass production technology. These two factors hold potential for further improvements of print quality in color and halftone applications.

Improving print quality in dot matrix printing means to minimize the digitizing effect by smaller, more accurate dots arranged in a finer grid. In thermal inkjet systems this means to improve the whole functional chain of energy transport from the driving pulse to the dot on the paper.

Accordingly drop-on-demand printing requires higher uniformity of the droplets (mass, speed and directionality). The uniformity is represented by mean values and standard deviations of drop mass and speed measured within one printhead.

In this paper effects of different heater surfaces and driving pulses on local and temporal uniformity of the vapor bubble within a printhead are investigated. A stable and uniform bubble generation is a necessary requirement for good print quality.

## Method

The BJ principle is characterized by the bubble formation. Functional connection between the expelled ink drop and bubble is given in approximations (1) to (3):

$$v_d \sim m_d \quad (1)$$

$$m_d \sim V_b \quad (2)$$

$$V_b \sim L_b \quad (3)$$

with drop velocity ( $v_d$ ), drop mass ( $m_d$ ), bubble volume ( $V_b$ ) and bubble length ( $L_b$ ). Figure 1 is a block diagram of a BJ module. It shows mutual relationships between components of the fluid path. Every single block attenuates the pressure signal. If a multitude of heaters is actuated simultaneously hydraulic crosstalk via ink reservoir overlays the pressure signal in any individual ink channel. This affects the uniformity of ejected ink drops.

---

Originally published in *Proc. of IS&T's Ninth International Congress on Advances in Non-Impact Printing Technologies*, October 4-8, 1993, Yokohama, Japan.

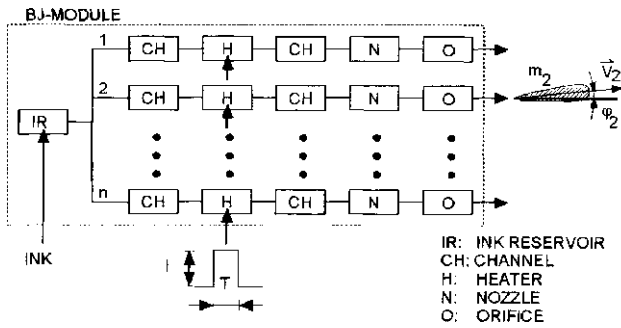


Figure 1. Block diagram of bubble-jet module

According to approximations (1) and (2) the two major characteristics of an ink drop—mass and speed—can be derived from the vapor bubble. Optimization of drop uniformity hence starts with actuator and drive input pulse. To exclude the above mentioned impacts on the individual bubble some premises must be observed:

- (a) While measuring only one heater is actuated.
- (b) The measurements are done under open pool conditions<sup>3</sup> on BJ modules without ink channels (see Figure 4).
- (c) Restriction on opaque or transparent test fluids to assure visibility of the bubbles.

The theoretical background of the bubble generation process was discussed in various papers. The works of Hsu<sup>4</sup> and Runge<sup>5</sup> stand in for it.

Hsu finds the size range of active nucleation centers being determined by surface-to-bulk temperature, thus emphasizing a strong effect of heater surface on the boiling process. High heat fluxes activate a higher number of different sized cavities as nucleation centers than low heat fluxes do. For that reason film boiling will occur earlier with drive input pulses of high power than with low power pulses. Therefore a high power pulse results in smaller bubbles meaning lower efficiency.

According to Runge liquid to vapor phase change is only determined by maximum temperature of interfacial layer and local temperature gradient. He regards the boiling process as largely independent of layer properties. Interfacial layers with low temperature gradients are found to be most effective in terms of efficiency, that is form larger bubbles. Time-delay between leading edge of driving pulse and first nucleation on the thin-film heater is regarded as the ‘most important quantitative measurable property of the bubble formation process’.

Since duration of the waiting period is in the range of 1 μs accurate measurement is very delicate and subject to measurement errors. To describe uniformity of bubbles within different BJ modules waiting time therefore is of limited value. Investigation of the state of maximum bubble growth proved to be a more suitable approach for the following reasons:

- Formation time of a maximum bubble can be observed with greater accuracy. It shows good correlation with bubble length.
- Temporal and local variations of a maximum bubble

- represent stability of the bubble formation process.
- Volume of the vapor bubble is a measure for efficiency of energy transport from heater to fluid.
- Approximation of bubble volume by bubble length allows easy measurement.
- Besides that bubble properties—including temporal behavior—are clearly connected with the ink drop (see approximations (1) to (3)).

Figure 2 shows two vapor bubbles at maximum extent in an open pool environment. (a) indicates a bubble in optimum, (b) in irregular shape. Regular shaped bubbles show high temporal stability, irregular ones tend to jitter. Type (b) occurs when additional bubbles of smaller size interfere with the main bubble. That is when boiling conditions are not homogeneous for the whole heated area. Since both bubble types often can be observed on adjacent heaters within one BJ module under definitely equal actuating conditions heater surface deserves special consideration.

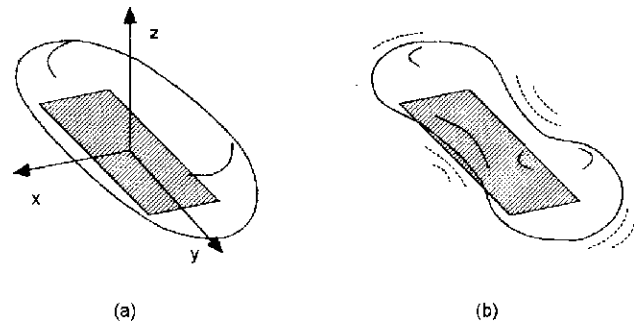


Figure 2. Maximum vapor bubble with optimum (a) and irregular (b) shape

The following equations characterize an optimal bubble of maximum extension:

$$V_{b,n}(x, y, z) = V_{b,max} = \text{const.} \quad (4)$$

$$\partial V_{b,n} / \partial x = \partial V_{b,n} / \partial y = \partial V_{b,n} / \partial z = 0 \quad (5)$$

$$\partial V_{b,max} / \partial t = 0 \quad (6)$$

$$n = 1, 2, \dots, m$$

(x, y, z - local coordinates, n - heater number, m - total number of heaters in BJ module).

When equations (4) to (6) are met under constant driving conditions bubble formation within a BJ module is regarded even. Standard deviation of the bubble lengths stands for uniformity of bubble growth. The mean value of bubble lengths is determined by physical properties of the heater material composition.

The heater elements are actuated by square-wave pulses of defined duration. Measurement is performed at threshold pulse energy, the energy value necessary to reach maximum bubble size. A further increase of pulse energy does not yield larger bubble size or efficiency as Figure 3 shows. So a further assumption for bubble uniformity measurements is:

(d) Pulse energy  $\geq$  threshold (pulse) energy.

For pulse durations smaller than phase change durations energy transfer to the ink is most effective<sup>5</sup>.

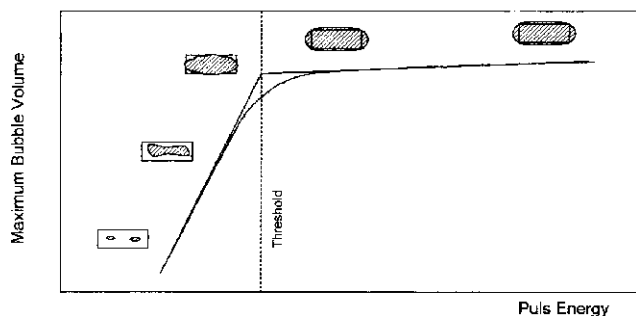


Figure 3. Qualitative characteristic of maximum bubble volume versus pulse energy

To keep results of different layer systems comparable measuring time per heater in uniformity experiments was limited to a few minutes. This is to avoid any sort of surface modification through operation as far as possible which could dominate the bubble behavior, like for instance kogation, cavitation defects, uneven etching on the heater by the fluid do<sup>6,7,8</sup>. For that reason the same test fluid was used in the uniformity experiments.

## Experimental

Figure 4 schematically shows the open pool test set-up. Its components are: Liquid pool, contacting device for the BJ module, viewing microscope, video system, drive circuit, stroboscope, time-delay circuit and storage oscilloscope.

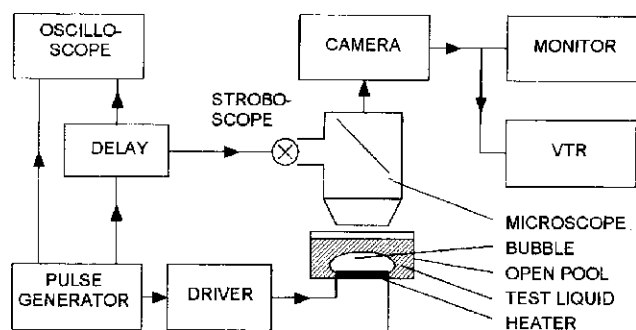


Figure 4. Schema of the open pool test set-up

With respect to bubble volume the chosen liquid volume in the open pool has to be regarded infinite. Bubble formation can be observed in x,y-plane (see Figure 2) at any state of emergence by the time-delay circuit. Driving pulse and strobe are synchronized. For measurement of pulse duration and amplitude the storage oscilloscope is used. Power and energy of driving pulses are calculated from individually measured actuator resistances and pulse currents. The operation fre-

quency was kept constant for all measurements. For every single actuator threshold energy was individually adjusted. Bubble lengths are determined from the enlarged video screen images of maximum sized bubbles ( $L_b = |y|$  in x,y-plane, see Figure 2). Only shape and temporal behavior of the bubbles were recorded qualitatively during time of measurement.

Setting values in detail were: Pulse duration T:  $1.3 \mu\text{s} \leq T \leq 7.3 \mu\text{s}$  /  $1.8 \mu\text{s}$  (pulse 1) /  $3.7 \mu\text{s}$  (pulse 2), operation frequency  $f = 1 \text{ kHz}$ , number of active heaters  $n = 1$ , measuring time per actuator  $t = 2 \text{ min}$ . The test fluid was composed of 80% water, diethylene glycol and other additives.

Table I shows the tested heater surfaces or BJ module variants. Heater size was the same among all sample types (length  $158 \mu\text{m}$ , width  $35 \mu\text{m}$ ).

Table I. Heater Surface Properties

Sample No.	Material	Coating Type	Layer Thickness (nm)
1	$\text{Si}_3\text{N}_4$	PECVD	700
2	$\text{SiO}_2$	PECVD	200
3	SiC	PECVD	700
4	Ta	sputter PVD	600
5	$\text{TaO}_x$	anodic oxidation	200
6	Au	evaporation coating	100
7	Pt	evaporation coating	50

For the given range of pulse durations threshold energy, maximum bubble length and pulse power were determined in time intervals of  $0.5 \mu\text{s}$ . The measurement was done with sample number 1 for one heater (Table 1). Uniformity experiments were performed with 2 discrete pulse durations—pulse 1 and 2—for each BJ module. In each case 25 out of 50 heaters per module were actuated with pulse 1 the other 25 with pulse 2.

## Results and Discussion

Figure 5 describes the relations between pulse duration, threshold energy, maximum bubble length and pulse power. Values in the diagram are given in percent with respect to the individual mean value within the pulse duration range.

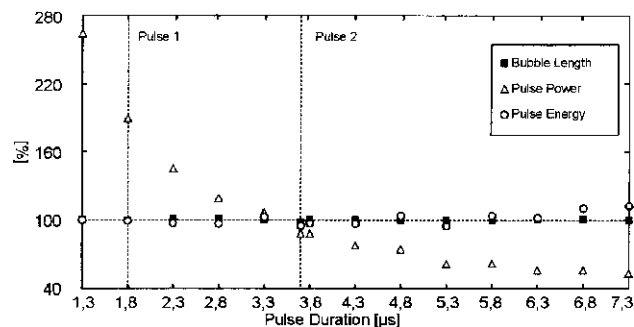


Figure 5. Maximum bubble length, threshold energy and pulse power versus pulse duration of a heater with  $\text{Si}_3\text{N}_4$  surface

While maximum bubble length and threshold energy remain constant pulse power rises by factor 5 from maximum to minimum value of pulse duration range. High pulse powers induce higher thermal stress in the heater thus having negative impact on the heater life<sup>6,8</sup>. Temporal stability of the bubble on the other hand decreases significantly from short to long pulse widths. For pulse durations < 3  $\mu$ s bubbles approach the state shown in Figure 2 (a). Long pulse widths create bubbles corresponding with Figure 2 (b). Optimization of BJ module performance by shorter driving pulses is limited by its correlation with heater life.

As noted above the following measurements are performed with two discrete pulses. They are indicated in Figure 5. Pulse 1 has about half the pulse width of pulse 2. Their difference in regard to power is factor 2.

Figure 6 summarizes the results for the heater samples of Table I. Mean values and standard deviations are shown relative to the mean value of the Ta sample (pulse 2).

The mean values express differences in efficiency of the various layer types. SiO<sub>2</sub> and Pt surfaces show higher Si<sub>3</sub>N<sub>4</sub>, TaO<sub>x</sub> and Au surfaces lower efficiency than Ta and SiC. Operation with high power pulse 1 tends to result in slightly lower mean values of bubble length than operation with low power pulse 2. This corresponds with the findings of Hsu<sup>4</sup> and Runge<sup>5</sup>. The only exception is the Au surface that shows contrasting behavior.

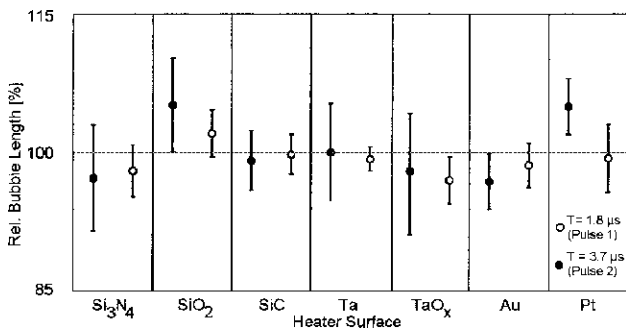


Figure 6. Mean values and standard deviations of maximum bubble length for driving pulses 1 and 2 measured in BJ modules with different heater surfaces

Regarding bubble stability clear differences between the two operation pulses exist. For operation pulse 2 standard deviation of bubble length is lowest with SiC, Au and Pt surfaces, highest with TaO<sub>x</sub>, Si<sub>3</sub>N<sub>4</sub>, SiO<sub>2</sub> and Ta surfaces.

All materials except the two evaporation coatings—Au and Pt—reveal remarkable improvement of bubble stability with high power pulse 1 as Figure 6 indicates. Sensitivity for pulse power is highest with Ta. In this case high power pulse 1 reduces standard deviation by 70% referring to low power pulse 2. The Au surface proved invariant to pulse power changes. With Pt standard deviation rises significantly with high power operation. This may be caused by inhomogenous layer properties originating in the evaporation coating process. In accordance with Hsu<sup>4</sup> improved temporal stability in

operation with high power pulses can be put down to a more homogeneous state of film boiling since the number of nucleation sites increase (see section ‘Method’)

In addition to the standard deviation temporal behavior of the individual bubble was valuated qualitatively. Table II shows the results.

Table II. Temporal Stability of Maximum Bubble

Sample No.	Material	Pulse 2 - T=3,7 $\mu$ s	Pulse 1 - T= 1,8 $\mu$ s
1	Si <sub>3</sub> N <sub>4</sub>	0	+
2	SiO <sub>2</sub>	—	0
3	SiC	0	+
4	Ta	0	+
5	TaO <sub>x</sub>	0	+
6	Au	++	++
7	Pt	+	+

Temporal stability (0) normal, (-) worse, (+) better, (++) much better

Highest temporal constancy of the maximum bubble was observed for Au surfaces with high and low power pulse alike. It shows good, SiO<sub>2</sub> poor temporal stability for low power pulse 2. All surface materials except Au respond clearly on an increase of pulse power with higher temporal stability. Figure 7 illustrates the influence of pulse power on bubble quality. For adjacent heaters within one BJ module maximum bubbles are shown. Upper row heaters were actuated with pulse 1, lower row heaters with pulse 2. Obviously performance is better in the upper row, that is for pulse 1.

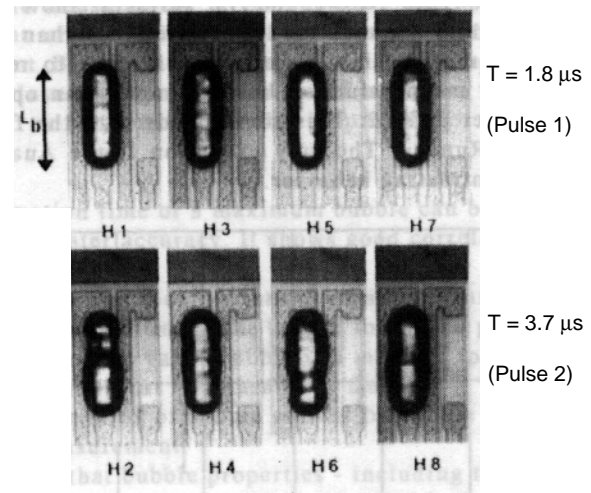


Figure 7. Bubble formation with pulse 1 and 2 on Ta heaters within one BJ module.

Out of the tested materials Au appears most favorable as heater surface. But as Pt has poor adhesion characteristics therefore both materials are not suitable for the use in commercial BJ printheads. The invariance of these two evaporation coatings to changes of pulse power make their surface properties most interesting for

further investigations. Both of them can serve as standards for qualifying other surfaces in respect to uniformity of bubble formation.

SiC also has the advantage of being (almost) independent from pulse power changes. Taking in account its temporal behavior it is the most over all suitable material for the heater surface.

For the other materials driving pulse power proves most effective for altering local and temporal bubble stability. Higher pulse powers mean higher thermal gradients in the heater and thus shorter heater life must be expected.

Amongst the tested materials bubble stability on Ta is most dependent on driving pulse power. As for  $\text{Si}_3\text{N}_4$ ,  $\text{SiO}_2$  and  $\text{TaO}_x$  only high power pulses guarantee a stable bubble formation.

All in all the observed differences in mean values and the standard deviations of the various heaters in a BJ module have to be considered small in the absolute (< 10%). Since the jitter of the individual bubble adds to the standard deviation it can result in detectable dot size variation and dot misalignment on the paper (see section 'Method'). For color and halftone printing with higher resolutions uniform performance of the printhead becomes more and more important and thus uniformity of the bubble formation process.

### Conclusion

It has been shown that bubble uniformity depends on heater surface and drive-input pulse. Uniformity of the bubble formation can be improved by shorter driving

pulses of higher power. This goes especially for Ta surfaces. Au and Pt can serve as standards for bubble uniformity measurements. Both materials are not suitable as passivation layers in commercial printheads. SiC surfaces show good efficiency and bubble stability. Stable and uniform bubble generation is a necessary but not sufficient condition for good print quality.

### References

1. M. Ikeda, "The Bubble Jet Printing Technology for BJ-80 Printer", *I.G.C. 18th Ann. Conf. Ink-Jet Printing*, Amsterdam **27-29.3.1985**.
2. R. R. Allen, J. D. Meyer and W. R. Knight. "Thermodynamics and Hydrodynamics of Thermal Ink Jets", *Hewlett Packard J.* **36.5**, (1985).
3. A. Asai, S. Hirasawa and I. Endo. "Bubble Generation Mechanism in the Bubble Jet Recording Process", *J. Imaging Tech.* **14** 120-124, (1988).
4. Y. Y. Hsu, "On the Size Range of Active Nucleation Cavities on a Heating Surface", *J. Heat Transfer* **84** (C) (1962).
5. W. Runge, "Berechnungsmodell thermischer Tintenschreibwerke", *Diss. München*, 11-55, 1992.
6. L. S. Chang, "Factors Influencing the Lifetime of Thermal Ink-Jet Heaters", *Dig. Tech. Pap. SID Int. Symp.* **18**, New Orleans LA. **12-15.5.1987**. Ed. J. Morreale. New York: Palisades, 192-195, 1987.
7. L. S. Chang, "Effects of Ink Decomposition on the Operation and Lifetime of Bubble Jet Thin-Film Heaters", *Proc. Japan Hardcopy*. Tokyo, 173-176, 1988.
8. L. S. Chang, "Mechanisms of Failure of Thermal Ink-Jet Thin-Film Heaters in Alkaline Solutions", *Dig. Tech. Pap. SID Int. Symp.* **19**. Anaheim CA. **24-26.5.1988**. Ed. J. Morreale. New York: Palisades, 271-274, 1988.